npj | climate and atmospheric science

Article

Published in partnership with CECCR at King Abdulaziz University

https://doi.org/10.1038/s41612-025-00951-y

Rapid decline and mortality of a Pleistocene-aged forest now submerged in the northern Gulf of Mexico, USA

Grant L. Harley[1] ✉, Kristine L. DeLong[2,3], Marcus Lofverstrom[4], Carl Andy Reese[5], Ellen V. Bergan[1], Samuel J. Bentley Sr.[3,6], Kehui Xu[3,7], Kelli Moran[3,7], Karen E. King[8] & Alicia Caporaso[9]

The Gulf and Atlantic Coastal Plains of the southern United States are characterized by a wide continental shelf that was subaerially exposed for ca. 80,000 years during glacial-interval marine regressions and transgressions. Given their present submergence, little is known about the vegetation dynamics, particularly at annual time scales, of these formerly terrestrial sites due to erosional processes associated with marine transgressions. Here, we present an annually resolved and well-replicated 489-year tree-ring chronology from macrobotanical specimens—anatomically identified as *Taxodium distichum* (L.) Rich.—collected in situ from a recently exposed submerged forest in 18 m water depth in the northern Gulf of Mexico. This chronology not only reveals historical vegetation dynamics at annual resolutions during Marine Isotope Stages 3–5a, but it also captures a catastrophic mortality event likely connected to intense storm activity, perhaps driven by freshwater fluxes from Heinrich events. Our findings are supported by coupled climate model simulations from the last glaciation, providing new insights into the environmental history of the southeastern US coastal regions.

The southeastern region of the United States of America (USA) is characterized by a wide continental shelf (~100–1000 km) that was exposed for as long as ca. 80,000 years during glacial-interval marine regressions[1,2]. As local ecosystems shifted seaward, this newly uncovered land became inhabited by plants and animals, similar to other well-known sites, e.g. Beringia[3], Doggerland[4], and Sundaland[5]. Marine transgression after the Last Glacial Maximum (LGM; after ca. 20,000 ka) either removed by erosion or buried these formerly terrestrial sites in the offshore marine environment.

Hurricane Ivan made landfall as a strong category 3 storm at Gulf Shores, Alabama, USA on 16 September 2004. Shortly afterwards an area of previously buried logs and tree stumps rooted in their growth position was found 13 km off the coast in 18 m water depth (Fig. 1B; hereafter termed submerged forest). Geophysical surveys found an elongated depression ~100 m long and about 1.0 m deep in the seafloor trending northwest to southeast[6,7]. This depression was likely a result of substantial bottom scour made by Hurricane Ivan, as similar scouring was documented in nearby locations[8,9]. Divers found more than 50 well-preserved tree stumps and logs in and around the depression that were visually identified as most likely being *Taxodium distichum* (L.) Rich. by their iconic knees and buttresses[10], however, not yet confirmed with wood anatomical analyses.

Preservation of the wood at the site was made possible by the anoxic conditions created by subsequent burial, which limits biological organisms and slows decomposition[11]. Wood has been found in anoxic peat bogs in freshwater environments[12–15], but discovery of well-preserved macrobotanical specimens in the marine environment is rare because shipworms and other bioeroders quickly colonize and consume wood once uncovered[16]. The wood specimens collected by divers that were exposed from the sediments contain more marine boring organisms than those recovered from inside the sediment ledge. Some pieces of wood recovered from the sediment ledge by divers still had bark and beetle chambers were visible suggesting quick burial[6]. Overall, the wood collected by divers is well-preserved and radiocarbon dates of >43,500 BP reveal these deposits are from the Late Pleistocene when sea level was lower than today[6]. Now that the site is exposed, shipworms and other marine bioeroders are attacking the

[1]Department of Earth and Spatial Sciences, University of Idaho, Moscow, ID, USA. [2]Department of Geography and Anthropology, Louisiana State University, Baton Rouge, LA, USA. [3]Coastal Studies Institute, Louisiana State University, Baton Rouge, LA, USA. [4]Department of Geosciences, University of Arizona, Tucson, AZ, USA. [5]School of Biological, Environmental, and Earth Sciences, University of Southern Mississippi, Hattiesburg, MS, USA. [6]Department of Geology and Geophysics, Louisiana State University, Baton Rouge, LA, USA. [7]Department of Oceanography and Coastal Sciences, Louisiana State University, Baton Rouge, LA, USA. [8]Department of Geography and Sustainability, University of Tennessee, Knoxville, TN, USA. [9]US Department of the Interior, Bureau of Ocean Energy Management, New Orleans, LA, USA. ✉e-mail: gharley@uidaho.edu

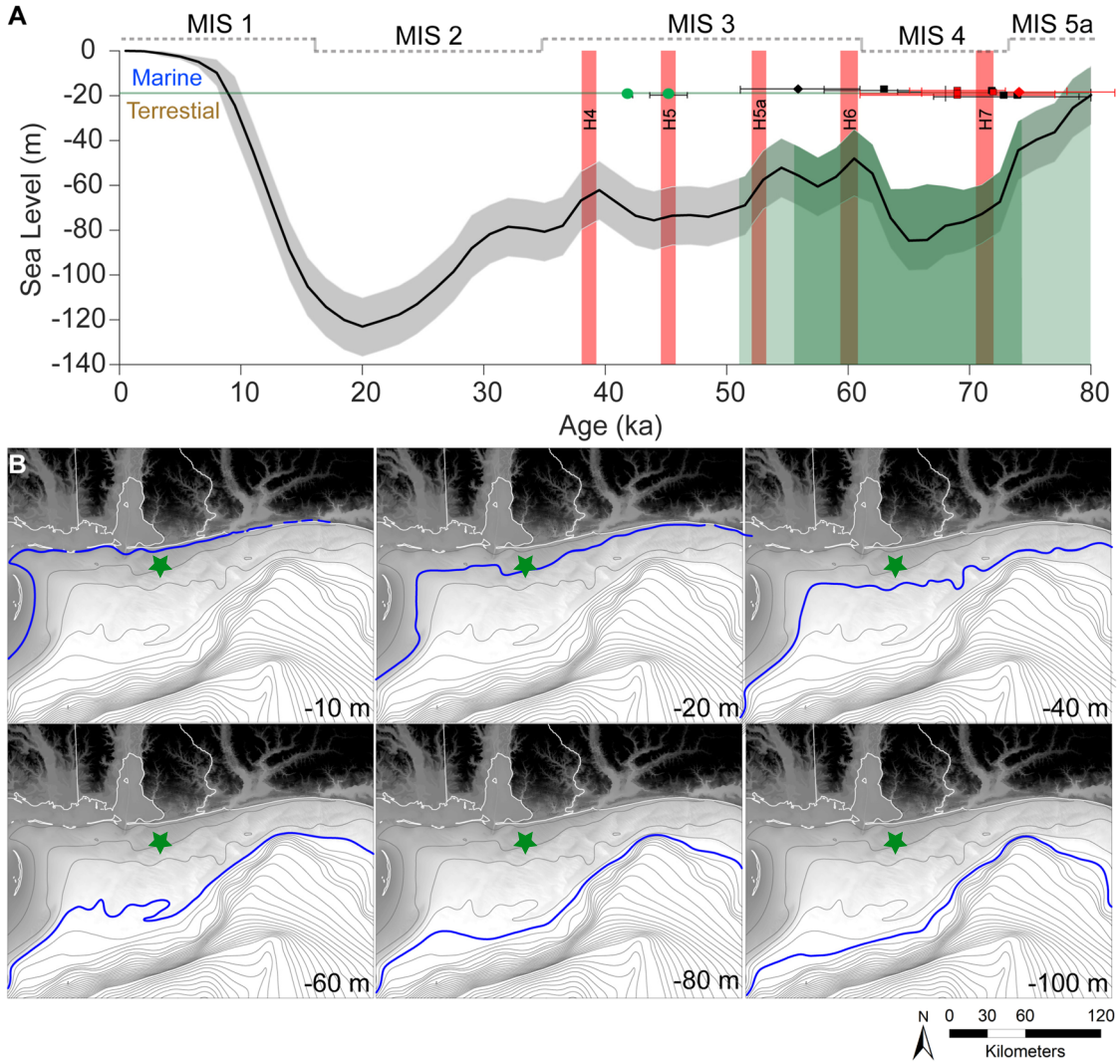

Fig. 1 | Submerged forest site setting within the northern Gulf of Mexico, USA. **A** Global sea level relative to the present day for the past 80 ka (black line) with estimated maximum and minimum sea level (gray shaded[24]). The age range for the submerged forest site shown in green shaded region and is based on prior (black squares/diamonds)[6] and new (red squares/diamonds) optically stimulated luminescence (OSL) dates[21]. Squares are OSL samples from late Pleistocene interbedded mud and peat (LPIMP) facies where wood was found and diamonds are paleosol facies that do not contain wood. Radiocarbon dates from organic debris in LPIMP are green circles[6]. Marine Isotope Stages (MIS) 1–5a (dashed gray) are based on Railsback et al.[87] and are plotted with Heinrich events (vertical red[88]). The current position of the submerged forest site is denoted with a horizontal green line at ~18 m water depth. **B** Estimated coastlines (blue) for past sea level (using modern bathymetry as a proxy; isobath interval = 10 m) relative to the location of the submerged forest site (green star). The submerged forest site is located ~13 km offshore of Gulf Shores, Alabama, at ~18 m water depth on the outer-continental shelf. See Fig. S1 for a broader geographical view of site location.

exhumed wood[17–19], and the exposed stumps will eventually be lost to decay. Our previous studies[6,20] found the diver-collected wood samples were radiocarbon dead (e.g. older than 43,500 BP), and the muddy-peat sediments containing woody remnants in sediment cores from the site were dated between 74 ± 6 and 61 ± 7 ka (2σ) (Late Pleistocene) using optically stimulated luminescence (OSL)[6,21] (Fig. 1). The now submerged forest was alive when sea level fell in response to ice sheet expansion during the Wisconsin glacial episode or Marine Isotope Stage (MIS) 3 and 5a (57–82 ka)[6]. Using modern coastal bathymetry[22,23] and global sea-level variations[24] (because no regional sea level histories are available), we posit this site was ~50–100 km inland when the forest was alive at an elevation between 20 and 80 m, varying within dating uncertainties[6] (Fig. 1). We interpret the location of the forest as being tectonically stable (~2.3 m subsidence/10 ka)[25] and any potential leveraging associated with the Laurentide Ice Sheet are less than the potential elevation of the forest.

Previously Reese et al.[20] conducted a pollen analysis of the Pleistocene-aged muddy-peat sediments at the site and found *T. distichum–Nyssa aquatica* backwater forest assemblages similar to modern-day southeastern US swamps that transition to an Atlantic Coastal Plain Blackwater Levee/Bar Forests, of which the closest analog today is located along coastal North and South Carolina[20]. The final transition in the pollen record, located near the top of the muddy-peat sediments, was to a grass and sedge-dominated environment that was likely a brackish or salt marsh[11]. Other pollen studies suggest that the coastal plains of the southeastern USA were dry during glacial intervals[26–30], yet these submerged trees suggest that robust coastal wetlands were present during the early period of the last glacial interval[20].

Here, we present an annually resolved and well-replicated tree-ring chronology from macrobotanical specimens collected in situ from the submerged forest (submerged forest chronology; SFC). Little is known about the vegetation dynamics—particularly at annual time scales—of former terrestrial sites along the northern Gulf of Mexico due to erosional processes associated with marine transgression. This new record provides a glimpse into the short- and long-term vegetation growth trends along the Gulf of Mexico continental shelf during MIS 3–5a. The end of the record captures a catastrophic event that caused widespread mortality at the site. Using coupled climate model simulations during the last glaciation

combined with the interpretation of the tree-ring record, we show that the most likely mortality agent was a strong storm, which at the time was primarily controlled by freshwater fluxes associated with Heinrich events.

Results

Species identification

Observations during the diving expedition suggested the species of most of the stumps at the submerged forest site to be *T. distichum* based on the iconic basal buttress swell and abundance of pneumatophores (e.g. *T. distichum* knees) that were scattered throughout the site positioned adjacent to stumps. After examining the wood specimens collected from the site, we found the primary cellulose structure intact on most samples with no visible indications of permineralization (Fig. 2A–E). Wood specimens that were fully exposed from the sediments contained more marine boring organism galleries compared to those recovered from inside the sediment ledge along the depression. Some wood pieces recovered from the sediments still contained bark and beetle chambers intact, suggesting quick burial and excellent preservation. Examination of the wood specimens under light microscope confirmed the wood type to be conifer, but a confident species identification based solely on cellular characteristics on the transverse plane was difficult because the growth-ring anatomy of *T. distichum* and *Chamaecyparis thyoides* (L.) Britton, Sterns & Poggenb. are indistinguishable[31]. *C. thyoides* is another Cupressaceae species also distributed along the Gulf Coast and is also indistinguishable from *T. distichum* in the palynological record, as noted by Reese et al.[20]. Several microanatomical characteristics, most notably the presence of longitudinal parenchyma visible in the transverse, tangential, and radial planes of the submerged forest specimens (Figs. S6 and S7) and confirmed with modern samples of *T. distichum* (Fig. S8) and *C. thyoides* (Fig. S9), helped us confirm the observations made by divers that the wood specimens retrieved from the submerged forest site were *T. distichum*[31]. Further, we were able to determine that specimens were not members of the Pinaceae family, due to the lack of resin canals and longitudinal parenchyma in the tangential plane[31].

SFC growth trends and modern analog

After drying, we excluded wood specimens that appeared to derive from roots or branches, and only retained samples that were confirmed by divers to be derived from in situ stumps or large sections of stumps lying on the surface sands and sediments ($n = 12$). Two of the 12 specimens retained for dendrochronological analysis could not be successfully crossdated due to issues with poor circuit uniformity and disturbance from marine boring organisms. We successfully crossdated a total of ten samples against each other to develop a tree-ring chronology that was not anchored in time (e.g. "floating"; Table S1). The SFC spanned 489 years in length with series intercorrelation of 0.61 ($p < 0.001$), RBAR of 0.42, and mean tree age of 312 years (Fig. S2; Tables S1 and S2).

Mapping the Gini coefficients for the 39 *T. distichum* time series distributed throughout its modern geographic range revealed noteworthy patterns of growth trend diversity compared to the SFC (Fig. 3). When comparing the SFC to the closest modern analog, the SFC (Gini = 0.24) growth trend was the most similar to a modern *T. distichum* chronology from the Pascagoula River, Alabama, USA (PASC; Gini = 0.23), with a difference in Gini of 0.016 (Table S2). Further, *T. distichum* individuals located at the southwestern range limit in Texas, the southern range limit in

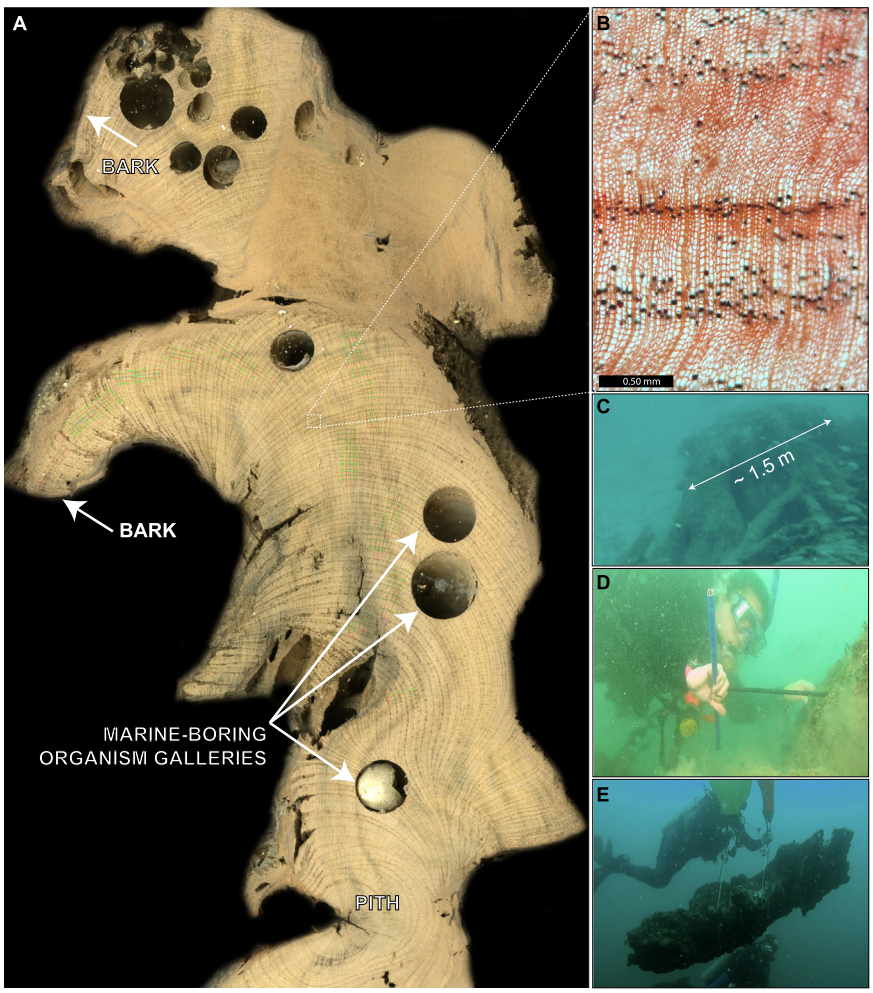

Fig. 2 | Representative *T. distichum* cross section from the submerged forest, northern Gulf of Mexico. Scanned image of submerged forest macrofossil specimen **A** shown with bark, pith, and galleries caused by shipworms burrowing into the wood after exposure to the marine environment. Inset images show **B** a microanatomy thin section with earlywood and latewood tracheids of the *T. distichum* specimen and photographs showing the **C** in situ stumps and the various methods used by divers to collect specimens via **D** hand-held increment borers and **E** lift bags.

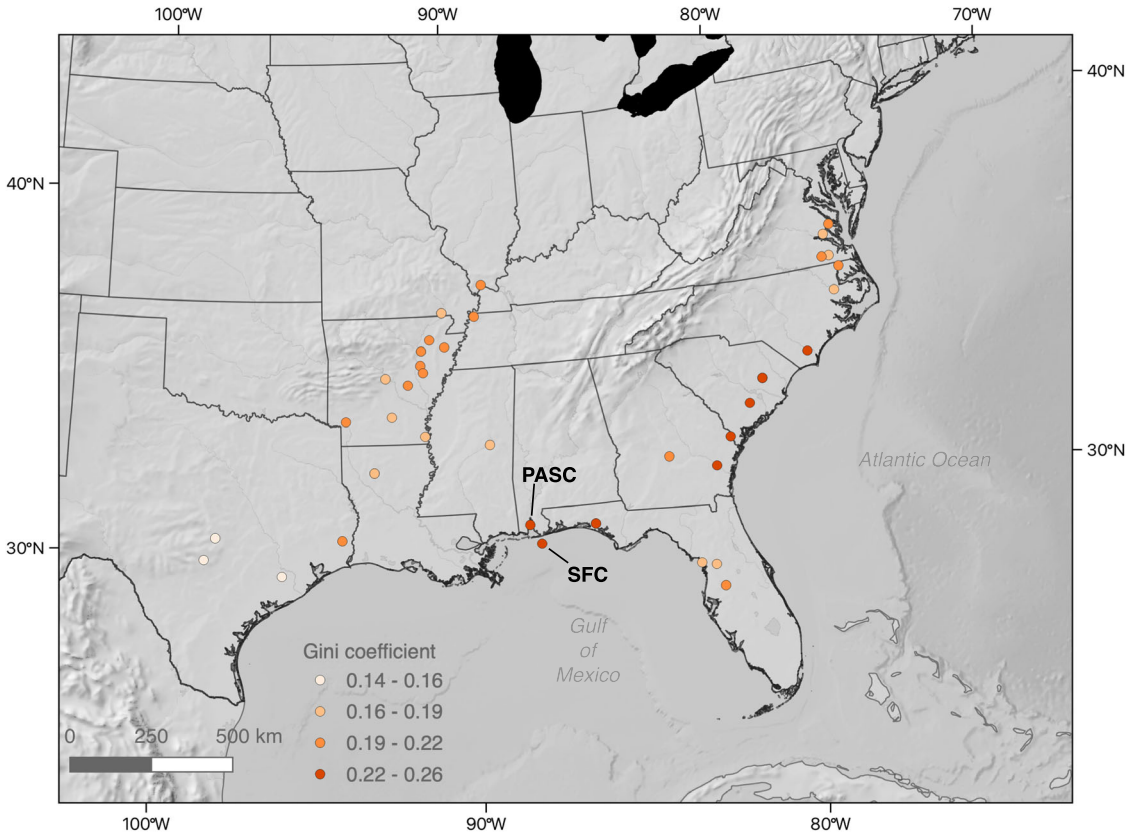

Fig. 3 | Inequality of SFC growth trends compared to modern analogs. Map showing the distributions of Gini coefficients of the publicly available *T. distichum* chronologies throughout the species geographic range ($n = 39$) and locations relative to the SFC in the northern Gulf of Mexico. All publicly available records accessed at the NOAA International Tree Ring Data Bank.

Florida, along the Mississippi River Valley, and the northern latitudinal range limit in North Carolina and Virginia were characterized by the most dissimilarity to the SFC. Although separated in time, trees that exhibited the highest similarity (smallest difference in Gini) are located in close proximity to SFC along the Gulf and Atlantic Coastal Plains, including PASC. This suggests that similar climatic limiting factors on tree growth characterize the SFC as with PASC and other coastal chronologies[32,33]. Spectral analysis of the SFC time series (Fig. 4) over the period relative years (RY) 100–489 identified periodicities in the time series that are significantly different from a red-noise assumption in the interannual (2–3 yr; $p < 0.05$–0.01) and at centennial to multidecadal periodicities ($p < 0.01$) (Fig. 4B). The same analysis revealed similar frequency patterns for the PASC chronology (Fig. 4E) spanning the period 1466–1992 CE for interannual and centennial to multidecadal periodicities ($p < 0.01$) (Fig. 4F). Mortlet wavelet analysis indicated that the interannual frequency in the SFC was present throughout most of the time series, from RY 100 to RY 350 (Fig. 4C, G). Yet, after RY 350, the interannual frequency fades contemporaneously with the gradual decline in growth, a pattern which is most likely associated with growth conditions that were slowly becoming more adverse. The derivative of Gaussian wavelet, which is more appropriate for capturing events (but not oscillations) reveals events that span 16-yr, 60-yr, and 250-yr exist throughout most of the SFC record, with more events during the terminal 100 years of the lifespan of the trees compared to the previous ca. 350 years (Fig. 3D, H).

After comparing the growth trends between the SFC and PASC, a notable difference between the two records was the rapid decline in growth at the end of the SFC that is absent in the PASC record. To investigate the temporal variability of ring-width diversity among measured series in the SFC record, we calculated the Gini coefficient in 100-yr intervals and assessed the rolling variance (Fig. S3A, B). Tree-ring diversity (i.e. sensitivity) steadily decreased from 0.23 to 0.14 during the first 400 years of the record, then increased sharply to 0.36 from year 400 to the end of the record at RY 489. We also note a substantial increase in variance in growth between SFC trees during the last ca. 100 years of the record (Fig. S3B). We interpret this change in temporal ring-width diversity and increased variance to be representative of a series of events that likely caused physiological stress to individual trees and eventually led to the rapid decline of multiple individuals at the site. This sudden change from more stabilized growth variability to a period of erratic growth, not only within individual trees but also between them, can also be seen in the plot of ten raw ring-width measurements that make up the SFC (Fig. S4).

Discussion

T. distichum is an iconic tree of the humid subtropical southeastern USA and is an indicator species for coastal wetlands and swamps at elevations <120 m, but most individuals growing under the current climate regime are found at <50 m[34–38]. As the longest-lived tree species in the southeastern USA[39], *T. distichum* has been widely used for climate reconstruction by using dendrochronology[40–42]. Given the species occupies rivers, floodplains, and swamps, individuals are able to withstand flooding events and moderate amounts of salt intrusion but do not grow in brackish or saline waters[43,44]. Though at such low elevations (<50 m), *T. distichum* can occur close to coastlines and their mild salt tolerance—compared to other species—allows them to survive modest pulses of saltwater such as storm events[43,44]. On longer time scales, *T. distichum* is impacted by sea level rise as coastlines shift with marine transgressions and regressions especially on glacial-interglacial time scales when global sea levels fluctuated by ~125 m[24]. Swamps occur in depressions that provide accommodation space for sediments to bury the

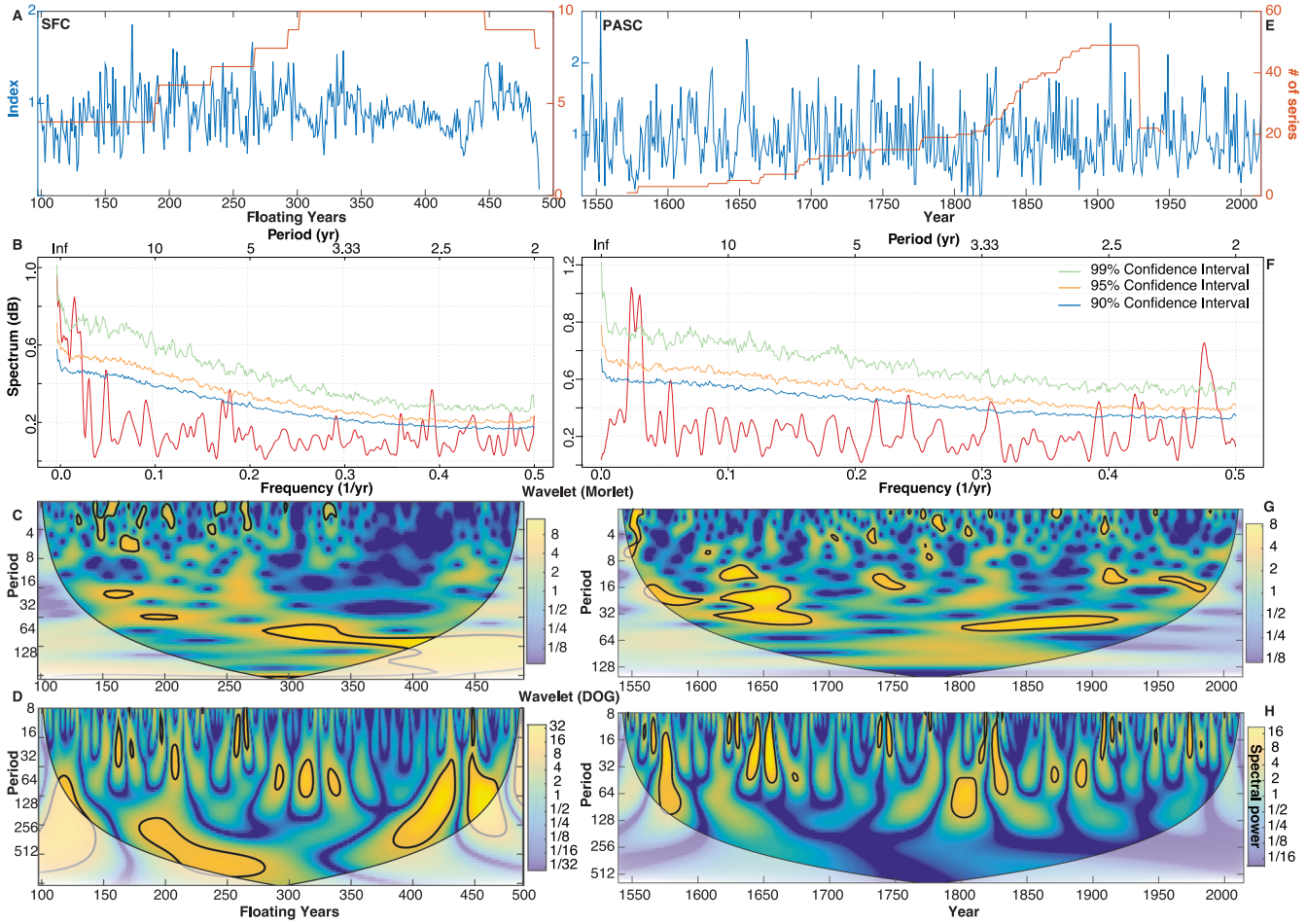

Fig. 4 | Times series comparisons of the submerged forest chronology (SFC) and modern *T. distichum* chronology from the Pascagoula River, Alabama, USA (PASC). Plotted for the SFC (**A**) and PASC (**E**), respectively, are MTM spectra (**B**, **F**), Mortlet wavelets (**C**, **G**) and derivative of Gaussian wavelets (**D**, **H**). The SFC is truncated at relative year (cambial age) 100 due to EPS < 0.85[50] (Table S2). The full record can be viewed in Fig. S2.

forest with enough sediment to preserve the deposits even during lowstand erosional processes. Previous studies suggest rapid sea level rise occurring ~40 or ~60 ka provided opportunities for local floodplain aggradation to bury the forest thus preserving the wood[45].

We were unable to return a confident radiocarbon date for any of the wood specimens collected from the in situ stumps. However, findings from Delong et al.[6] suggest the forest existed between ca. 74 and 61 ka. In addition to the in situ stumps, sediment cores collected within the trough where stumps were exposed were radiocarbon dated using samples of woody debris extracted from nine intervals within the Pleistocene facies; all but two suggested ages of >43.5 ka[6,20,46]. Given the age constraints and limitations of ^{14}C dating, we therefore consider the radiocarbon results from this study as a minimum age estimate for the submerged forest site[20]. To help constrain the chronology of the site, sediments extracted from the study area were dated using optically stimulated luminescence (OSL; c.f. Rittenour[47]) to the period ca. 74–61 ka[6]. In combination with the OSL date range of the site presented by Delong et al.[6], other lines of evidence for this age range are based on (1) past relative sea level change in the Gulf of Mexico within the context of the site depth below current sea level (e.g. Waelbroeck et al.[24] (Fig. 1)), and (2) the modern biogeography of *T. distichum* placing the species generally within 0–50 m above sea level[34,35,38]. We infer that this is consistent with the forest having grown during a shift from the last interglacial (MIS 5)—during which sea levels dropped exposing the continental shelf and allowing vegetation to expand southward—into the MIS 4–MIS 3 transition, during which the Laurentide Ice Sheet advanced southward and climate shifted to colder and drier conditions of the LGM[48].

During the approximate period of widespread forest mortality at the submerged forest site (74–61 ka), a shift occurred from the last interglacial (MIS 5) into the MIS4–MIS 3 transition. At this time, as the Laurentide Ice Sheet advanced southward and climate shifted to colder and drier conditions[48], which could have stressed the trees, receding sea levels exposed portions of the continental shelf, which in turn would have facilitated species migration and range expansion to lower coastlines of what now is the USA Gulf Coast and where the trees of the SFC were found. We found no evidence of charcoal or fire scars in the wood and sediments that could have led to mortality. Furthermore, we found no evidence of disease (e.g. wood decay, spalding) or widespread insect infestation (e.g. insect galleries) in the wood.

Previous pollen studies suggest that the coastal plains region of the southeastern USA was dry during glacial intervals[26–30,49], yet a pollen assemblage profile from the terrestrial sediments extracted from the submerged forest indicates that robust coastal wetlands were present during the early period of the last glacial interval (MIS 3–4)[20]. The uppermost Pleistocene terrestrial sediments presented by Reese et al.[20] are dominated by grasses (Poaceae) and sedges (Cyperaceae) indicating a more open environment. These pollen assemblages suggest that early glacial forests along the Gulf Coast were similar to what exists currently. Interpreting higher-resolution vegetation dynamics (e.g. annual growth variability) from such environments is scarce. Yet, successful crossdating and chronology development from the submerged forest enables a rare chance to obtain information about vegetation responses to environmental changes.

Growth trends at the beginning of the SFC exhibited a high level of variability, but this is common in many tree-ring time series and is attributed

to a low number of samples (Figs. 4A and S2). Sample depth was low ($n = 1$) during the first 76 relative years (RY) of the chronology but increases to $n = 4$ at RY 98 (Fig. S2). This low sample depth precluded growth trend interpretations until RY ca. 100, at which time the expressed population signal of the record was >0.85[50]. The period RY 100–350 was characterized by high-frequency growth variability until after which trees demonstrated a gradual decline in growth trend and year-to-year variability to RY 430. An increase in tree growth occurred between RY 430–482, which is followed by a marked decline in growth. RY 489, the last complete ring in the chronology, is characterized by the narrowest growth ring in the entire time series. Further, eight of the ten samples contained the same outermost growth ring as revealed by the crossdating process, which was characterized by a partial growth ring during RY 490 of 4–10 rows of earlywood tracheids, indicating that mortality occurred early in the growing season (e.g. spring). Bark was not present on two of the samples, and this is evident in the drop in sampled depth ca. RY 450 toward the end of the chronology. Yet, we posit that the rapid decline in growth toward the end of the chronology combined with the finding that eight of ten samples contained the same outermost partial growth ring inside bark suggests that some early-season event resulted in synchronous tree mortality, at least for most of the individuals included in the submerged forest chronology.

Given the proximity of the SFC site to the mouth of the Mississippi River (~100 km from the current mouth), changes in Mississippi fluvial dynamics may have influenced the growth displayed in the SFC, especially toward the last ca. 140 years of growth. Yet, the site is located to the east of, and within closer proximity to, the Mobile–Tensaw River system, which could have had a more direct influence[25]. Along the middle and lower Mississippi Valley regions, buried slackwater deposits suggest the Mississippi was flowing below the present position during the last interglacial, with initial slackwater deposition occurring ca. 77 ka at the MIS 5a–4 transition[51–54]. Then toward the end of MIS 4, the Mississippi aggraded rapidly and transitioned to a braided regime to form the highest and oldest braid belt, the Dudley, by the period 64 ± 5–50 ± 4 ka. Reese et al.[20] hypothesize that the present-day Mobile–Tensaw River system also became braided during this time, as evident in a coeval surge in *Alnus* spp. pollen associated with the Blackwater Levee/Bar forest assemblage discovered in a sediment core from the SFC site. We posit that based on (1) the previously established relationship between increased salinity and *T. distichum* radial growth and (2) the growth trends during the last ca. 140 years of the SFC chronology that trees were responding negatively to gradual increases in saltwater intrusion, or variations in Mississippi River meltwater during the early growing season, which ultimately led to the rapid decline in growth and mortality of the trees before eventual burial.

The most notable aspect of the SFC record is the changing growth trends from RY 350 to the end of the chronology at RY 489 marked by synchronous mortality in RY 490. *T. distichum* is known to have the ability to survive prolonged periods of freshwater flooding. In addition, previous research has found the establishment and survival of seedlings to be moderately salt tolerant (e.g. Chabreck[55]). In a controlled experiment, *T. distichum* seedlings treated with a 3 g/l saltwater solution for 60 days displayed no significant effects on height growth, stomatal conductance, or net photosynthetic rate compared to seedlings treated with freshwater[56]. However, Conner[57] found 100% mortality of seedlings subjected to treatments of regular saltwater (10 g/l) flooding. Hence, the combined disturbance of saltwater and flooding (e.g. saltwater inundation) is considered to be detrimental to the survival of *T. distichum* (e.g. refs. 56–58). Coastal wetland areas along the southeastern US Coastal Plain and, more specifically, the Gulf Coast have been subjected recently to increases in flooding and saltwater intrusion due to the combined effect of land subsidence and human-induced climate change and subsequent sea level rise[59–61]. Krauss et al.[59] found a strong negative relationship between site salinity and tree height, basal area ($m^2\,ha^{-1}$), and individual tree basal area increment (BAI; $cm^2\,yr^{-1}$) within *T. distichum* forests in South Carolina, Georgia, and Louisiana.

The age of the submerged forest site precludes us from invoking coupled climate models to suggest possible causal mechanisms responsible for such a widespread mortality event. Despite this challenge, we use the most recent analog of the last glaciation (ca. 21–12 ka) for which we have transient simulations with a coupled Earth system model. As is shown in Fig. 5A-D, changes in ice sheet forcing, orbital variations, and greenhouse gases all have a relatively small effect on the kinetic energy associated with storms along the USA Gulf Coast. On the other hand, freshwater fluxes

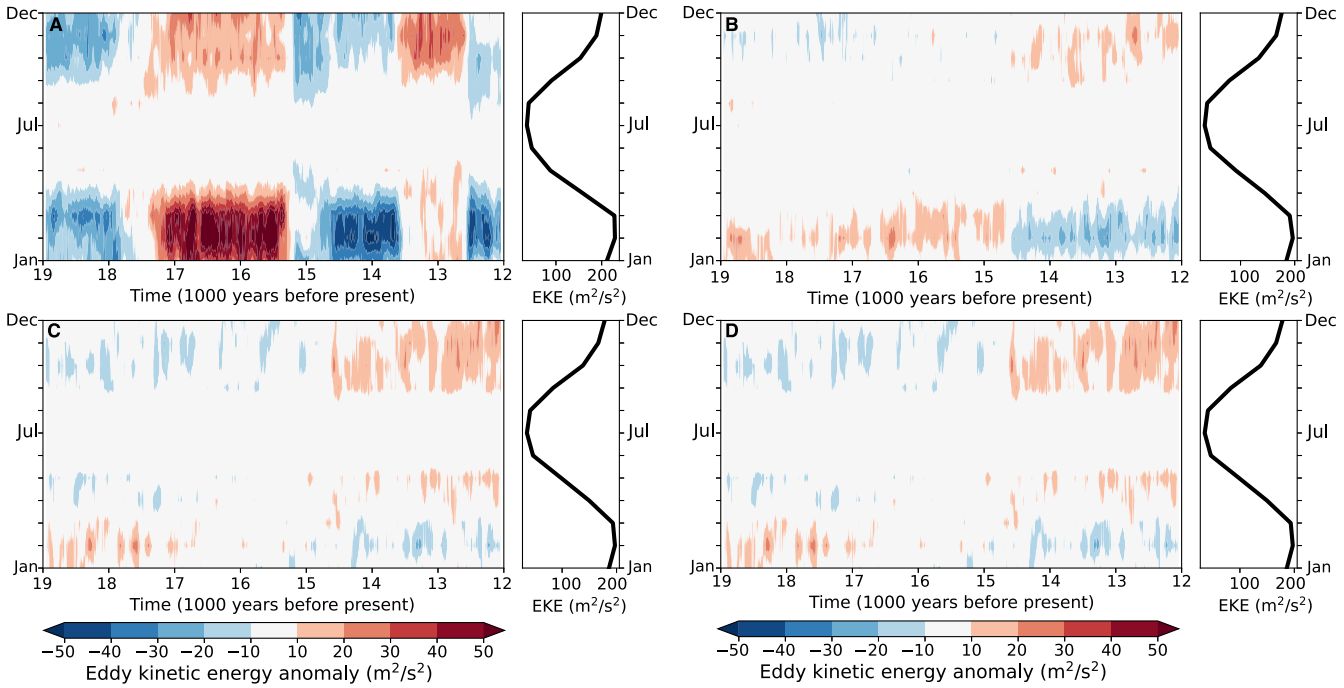

Fig. 5 | Coupled climate model simulations of storm activity freshwater forcing. iTrace model simulations of the last glaciations—from the Last Glacial Maximum (21 ka) to the end of glaciation (12 ka)—that demonstrate the isolated climate system response to changes in **D** ice sheets alone, **C** ice sheets + orbital patterns, **B** ice sheets + orbital patterns + greenhouse gas forcings, and **A** combined affect of ice sheet fluctuations, orbital patterns, greenhouse gases, and freshwater melt fluxes.

associated with Heinrich events have a large control on the strength of storms in the study area, including both tropical storms at the end of summer and winter storm tracks[62,63]. While this is not evidence that the trees were killed and/or buried by a large storm, an abrupt increase in the size of storms making landfall along the US Gulf Coast during Heinrich events is at least a plausible hypothesis for a stressor such as a flood event, prolonged saltwater inundation from storm surge, and ultimately burial of the trees, as Heinrich events were likely related to freshwater pulses causing rapid, regional flooding[48].

The North American Ice Sheet complex experienced large changes in size over the time period from ca. 72–52 ka. A recent reconstruction by Dalton et al.[48] suggests that the Laurentide Ice Sheet expanded from a spatially confined northerly state in the early MIS 4 (ca. 70 ka) to a much more spatially extensive state ca. 60 ka, followed by a partial retreat from 60 to 50 ka, coinciding with Heinrich Stadial 6 (ca. 60 ka). This Heinrich event is noteworthy as it marks an abrupt event (typical timescale of 500 ± 250 years) with a global climate signature[64] in the middle of the interval when the trees were alive. Our climate model simulations suggest that the storm activity along the US Gulf Coast increased substantially—including tropical cyclones—during Heinrich events (Fig. 5), supporting the hypothesis that the trees may have been buried by the surge or flood waters from an exceptionally large storm. An abrupt increase in the size of storms (and presumably saltwater inundation) could also help explain the stress the trees experienced for several decades before they abruptly died and were buried. In support of this theory, palynological, geochemical, and micro-fossil analyses from Reese et al.[20] and Fontenot et al.[11] show a clear transition from the Levee/Bar/Cypress Forest to open salt marsh.

Swamp environments, where *T. distichum* currently inhabits along the southeastern coastal plains of the USA, are characterized largely by stagnant waters with low oxygen content that provide favorable conditions for wood preservation[65,66]. Although with this study we were unable to provide an exact causal mechanism for the synchronous mortality and rapid growth variability at the end of the SFC record, we speculate that the most likely causes were either singular or combined events of drought, flood, and storm damage, which is consistent with model simulations of increased storm activity during Heinrich events. Another possibility for promoting wood preservation is rapid burial by a large volume of sediment from storm-induced river overbank flooding or marine transgression[67,68]. Heinrich[67] reported that two sites recently uncovered in situ along the lower Mississippi River in Louisiana, USA contained buried *T. distichum* stumps of 1.5 m height—similar characteristics to the submerged forest stumps—that would have required burial rates of 1.5–2 m in 100 years for preservation. Further, bark is generally shed first along with finer branches within the first few years following mortality of a standing tree[69], suggesting rapid burial of the submerged forest occurred, as suggested elsewhere in the region by Middleton[70,71]. The 489-year SFC record presented here provides a baseline on which to build future research at the site. Future work and subsequent sampling trips will be focused on (1) extending the length of the SFC chronology, and (2) investigating additional sites with preserved macrofossil wood that were recently discovered. These paleoenvironmental records will provide a better understanding of the dynamics of rapid sea level rise that occurred in the past, which can be used to inform coastal communities during this time of current and impending climate-induced sea level changes.

Methods

Field methods

During field campaigns in 2013, three teams of divers (two divers per team) worked in stages to acquire increment cores from the stumps using a hand-held increment borer (Fig. 2D, E). To ensure the acquisition of intact segments, the divers gave selection preference to specimens that exhibited the least amount of visible degradation[72]. Once samples were collected, they were sent to the surface in buckets with air-lift bags and floated to the research vessel. Samples were immediately tagged with a unique identification number and submerged in deionized water to prohibit desiccation and subsequent degradation. A total of 23 wood specimens were brought to the surface and transported back to the laboratory for analysis.

Species identification

Histological analysis of woody plants by observing their structural characteristics at the cellular level can identify wood to genus or species level in cases where macro-morphological assessment is not possible or is controversial (e.g. multiple species with identical transverse anatomical features[31]). Moreover, few woody plant species can be precisely classified solely on surface appearance; identification often entails examination of individual cells and cell walls across the different stem planes (i.e. transverse, radial, tangential; Fig. S5).

Certain microanatomical features are of particular diagnostic importance to distinguish between species and genera[20,73,74]. Alongside the qualities of latewood–earlywood cell transition in annual growth rings viewed along the transverse plane, features such as resin canals, longitudinal parenchyma, and subdividing end walls of tangentially viewed parenchyma cells can provide critical indicators of the identity of a wood specimen[31,73]. Palynological records and tree stumps from the submerged forest site provide critical baselines of the woody plant families, genera, and species. Namely, regionally occurring TCT species (e.g. *T. distichum*; *C. thyoides*), both of which are either noted in pollen records or identified by meter-scale observations of in situ specimens, are of particular interest in precisely identifying by their microanatomical features to confirm and/or qualify their occurrence in the paleocoastal environment of the northern Gulf of Mexico. The microanatomical features of *T. distichum* and *C. thyoides* are distinct enough to identify to genus and, when possible, species level (Table S3). Qualitative analysis of recovered woody plant material allows for a deeper, more precise insight into the species assemblages and coastal ecologies of the once-exposed portions of the outer-continental shelf that existing multivariate analyses of its paleoenvironmental settings are unable to distinguish.

For the anatomical assessment of the collected wood samples from the submerged forest, saturated wood specimens were placed in a fume hood and allowed to slowly dry to prevent cracking. Larger wood samples were cut into smaller pieces for the collection of thin sections. Samples were then cut to a thickness of 10–15 µm using a core microtome[75] from the transverse, radial, and tangential planes. The wood microsections sections were stained with a diluted safranin solution and mounted on glass slides following standard procedures for microscopic analysis[76]. Thin sections were then assessed with a Leica polarizing microscope at 4, 10, and 63× magnification for microanatomical features and characteristics. Identification of each wood specimen was made using diagnostic guidelines provided by Hoadley[31] and Esteban et al.[73].

Submerged forest tree-ring chronology (SFC)

In the laboratory, wood specimens were first placed in a fume hood and allowed to slowly dry to reduce cracking and checking. After drying, samples were mounted, then sanded using progressively finer sand paper and processed using standard dendrochronological methods[77]. Because exact calendar years of growth rings within the wood specimens were unknown, the innermost complete ring on each sample was assigned the relative year "1" and each subsequent 10th ring was marked with a "X" under the microscope. We then scanned each sample with an EPSON Expression 10000XL scanner and all tree-ring widths were measured to 0.001 mm accuracy using coupled CooRecorded/CDendro[78] software. We first used the computer program COFECHA[79] to help match and crossdate each sample relative to one other. We tested 40-year time segments lagged by 20 years to suggest possible temporal placements of all samples and used a minimum correlation value of 0.40 (typically $p < 0.001$) as a statistical standard of convincing agreement between measured series. After considering the suggested temporal placement made by COFECHA, we compared each series visually. Internal crossdating (or crossmatching) resulted in a set of measured series that were aligned temporally with each other "floating" in time, but not absolutely dated in time. Given that most samples

included pith and bark (Fig. 2), we then used ARSTAN to standardize each tree-ring series with a smoothing spline with a 50% frequency response cutoff equal to two-thirds the length of each series with variance stabilization[80]. This level of detrending preserves low-frequency variance in each series suitable for analysis of multidecadal growth trends.

Relative dating

Absolute dating of the submerged forest tree-ring chronology (SFC) is not possible because no reference tree-ring chronology exists for the Gulf Coast region that extends far enough back in time. Thus, we attempted to relatively date the wood samples collected during diving expeditions using radiocarbon dating techniques to better understand the temporal placement of the tree-ring chronology Delong et al.[6]. A total of nine wood samples collected by divers from in situ stumps were prepared and analyzed at the Center for Accelerator Mass Spectrometry (CAMS) at Lawrence Livermore National Laboratory. The radiocarbon dating results are reported in Delong et al.[6] (Table 2) and all wood samples were either radiocarbon dead or radiocarbon measurements were near the detection limits (i.e. older than 43,500 years). Therefore, radiocarbon dating was not useful in establishing the age of each wood piece. Therefore, a floating chronology is used, i.e. not fixed in time.

Paleo (SFC) vs modern (PASC) chronology comparison

We used a suite of techniques and analyses to compare the floating SFC with mod- ern analogs. For this, we first located the *T. distichum* tree-ring chronology that was the closest proximity to the SFC and publicly available via the NOAA International Tree-Ring Data Bank (ITRDB), which was from Pascagoula, Mississippi (PASC; 30.58° N, 88.02° W; Fig. 4E). The Pascagoula River chronology has ITRDB identification MS002 and was contributed by Stahle et al.[81]. The PASC *T. distichum* chronology spanned 484 calendar years from 1466 to 1992 CE. Second, to assess the inequality in the paleo record (SFC) vs modern analogs, we calculated the Gini coefficient[82], an all-lag measure of ring-width variability within each time series. We calculated Gini for the SFC, as well as all bald-cypress tree-ring chronologies within the species geographic range available on the ITRDB ($n = 39$, including PASC). Further, we used the redfit function in dplR package in R[83] to investigate the frequency domain and spectral aspects of the SFC and PASC. We complemented the spectral analysis by constructing wavelet spectra plots using Morlet (isolates low-frequency cycles with 1–3 cycles present) and derivative of Gaussian (DOG; isolates high-frequency events and not cycles) mother wavelets to examine how the modes of variability change with time within each time series[84,85].

Coupled climate model simulations

To the best of our knowledge, there are no model simulations with a comprehensive, coupled climate model of the 74–61 ka time period (when the trees were alive at the submerged forest site). As the best-available analog, we analyze the iTrace simulations, e.g.[86], which is a set of transient, fully coupled model simulations of the last deglaciation, from the LGM (21 > ka) to the end of the deglaciation (12 ka). iTrace consists of four simulations with the Community Earth System Model, version 1 (CESM1) that isolate the climate system response to changes in: ice sheets, orbital parameters, greenhouse gases, and freshwater fluxes. While the last deglaciation is not a perfect analog for the MIS 5–MIS 3 time interval, it nevertheless shares several aspects that may be useful for understanding the role of various climate-forcing agents. For example, the Laurentide Ice Sheet receded from its largest extent in the last glacial period (around 21 ka) to a comparatively small remnant ice sheet confined predominantly to northeastern Canada (broadly consistent with the interval from 60 to 50 ka[48]). The 8000-year interval simulated in iTrace covers about 1/3 of a precessional cycle, as well as Heinrich event 1[64] and the Younger Dryas (13.5–11.9 ka), both characterized by abundant freshwater fluxes into the North Atlantic and a partial return to glacial conditions.

Data availability

No datasets were generated or analyzed during the current study.

Received: 9 October 2024; Accepted: 12 February 2025;
Published online: 20 February 2025

References

1. Anderson, J. B. et al. Late Quaternary stratigraphic evolution of the northern Gulf of Mexico margin: A synthesis. In *Late Quaternary Stratigraphic Evolution of the Northern Gulf of Mexico Margin* (Anderson, J. B. & Fillon R. H. eds) 1–23 (Society for Sedimentary Geology, 2004).
2. Sydow, J. & Roberts, H. H. Stratigraphic framework of a late Pleistocene shelf-edge delta, northeast Gulf of Mexico. *AAPG Bull.* **78**, 1276–1312 (1994).
3. Hopkins, D. M. Aspects of the paleogeography of Beringia during the late Pleistocene. In *Paleoecology of Beringia* (eds Hopkins, D. M. et al.) 3–28 (Academic Press, 1982).
4. Weninger, B. et al. The catastrophic final flooding of Doggerland by the Storegga Slide tsunami. *Doc. Praehist.* **35**, 1–24 (2008).
5. Bird, M. I., Taylor, D. & Hunt, C. Palaeoenvironments of insular Southeast Asia during the Last Glacial Period: a savanna corridor in Sundaland? *Quat. Sci. Rev.* **24**, 2228–2242 (2005).
6. Delong, K. L. et al. Late Pleistocene baldcypress (*Taxodium distichum*) forest deposit on the continental shelf of the northern Gulf of Mexico. *Boreas* **50**, 871–892 (2021).
7. Moran, K. L. et al. Storm-driven tree exposure and geomorphic change: predicting the distribution of preserved Late Pleistocene tree stumps on the outer Alabama continental shelf. *Mar. Geol.* 107402 https://doi.org/10.1016/j.margeo.2024.107402 (2024).
8. Wang, D. W., Mitchell, D. A., Teague, W. J., Jarosz, E. & Hulbert, M. S. Extreme waves under Hurricane Ivan. *Science* **309**, 896–896 (2005).
9. Teague, W. J., Jarosz, E., Keen, T. R., Wang, D. W. & Hulbert, M. S. Bottom scour observed under Hurricane Ivan. *Geophys. Res. Lett.* **33**, L07607 (2006).
10. Raines, B. The underwater forest. YouTube video, 27:18. June 22, https://www.youtube.com/watch?v=PKm0eRfFFfo (2017).
11. Fontenot, K. et al. Snapshots of coastal ecology using multiproxy analysis reveals insights into the preservation of swamp and marsh environments since the late Pleistocene. *Geochem. Geophys. Geosyst.* **25**, 2024–011489 (2024).
12. Stoll, P., Weiner, J. & Schmid, B. Growth variation in a naturally established population of *Pinus sylvestris*. *Ecology* **75**, 660–670 (1994).
13. Szumigalski, A. R. & Bayley, S. E. Decomposition along a bog to rich fen gradient in central Alberta, Canada. *Can. J. Bot.* **74**, 573–581 (1996).
14. Ramil-Rego, P., Mun˜oz-Sobrino, C., Rodr´iguez-Guiti´an, M. & G ´omez-Orellana, L. Differences in the vegetation of the North Iberian Peninsula during the last 16,000 years. *Plant Ecol.* **138**, 41–62 (1998).
15. Wheeler, B. & Proctor, M. Ecological gradients, subdivisions and terminology of north-west European mires. *J. Ecol.* **88**, 187–203 (2000).
16. Fojutowski, A. et al. Changes in the properties of English oak wood (*Quercus robur* L.) as a result of remaining submerged in Baltic Sea waters for two years. *Int. Biodeterior. Biodegrad.* **86**, 122–128 (2014).
17. Kirk, T. K. et al. *Biological Decomposition of Solid Wood* (Citeseer, 1984).
18. Cragg, S. M. et al. Vascular plants are globally significant contributors to marine carbon fluxes and sinks. *Annu. Rev. Mar. Sci.* **12**, 469–497 (2020).
19. Altamia, M. A. et al. Wooden steps to shallow depths: a new bathymodiolin mussel, *Vadumodiolus teredinicola*, inhabits shipworm burrows in an ancient submarine forest. *Deep Sea Res. I Oceanogr. Res. Pap.* **204**, 104220 (2024).
20. Reese, C. A. et al. Stratigraphic pollen analysis performed on a late Pleistocene cypress forest preserved on the northern Gulf of Mexico continental shelf. *J. Quat. Sci.* **33**, 865–870 (2018).

21. DeLong, K. et al. *Investigation of an Ancient Bald Cypress Forest in the Northern Gulf of Mexico Phase 2 Final Report*. Technical Report M20AC1000 (Bureau of Ocean Energy Management, New Orleans, LA, 2025).
22. Love, R. et al. The contribution of glacial isostatic adjustment to projections of sea-level change along the Atlantic and Gulf coasts of North America. *Earth's Future* **4**, 440–464 (2016).
23. Kuchar, J. et al. The influence of sediment isostatic adjustment on sea level change and land motion along the US Gulf Coast. *J. Geophys. Res. Solid Earth* **123**, 780–796 (2018).
24. Waelbroeck, C. et al. Sea-level and deep water temperature changes derived from benthic foraminifera isotopic records. *Quat. Sci. Rev.* **21**, 295–305 (2002).
25. Bartek, L. R., Cabote, B. S., Young, T. & Schroeder, W. Sequence stratigraphy of a continental margin subjected to low-energy and low-sediment-supply environmental boundary conditions: Late Pleistocene–Holocene deposition offshore Alabama, USA. In *Late Quaternary Stratigraphic Evolution of the Northern Gulf of Mexico Margin* (eds Anderson, J. B. & Fillon, R. H.) 29–49 (Society for Sedimentary Geology, 2004).
26. Delcourt, P. A. & Delcourt, H. R. The Tunica Hills, Louisiana-Mississippi: late glacial locality for spruce and deciduous forest species. *Quat. Res.* **7**, 218–237 (1977).
27. Delcourt, P. A. & Delcourt, H. R. Pollen preservation and quaternary environmental history in the southeastern United States. *Palynology* **4**, 215–231 (1980).
28. Delcourt, P. A., Delcourt, H. R., Brister, R. C. & Lackey, L. E. Quaternary vegetation history of the Mississippi embayment. *Quat. Res.* **13**, 111–132 (1980).
29. Delcourt, P. A. & Delcourt, H. R. Late-quaternary vegetational dynamics and community stability reconsidered. *Quat. Res.* **19**, 265–271 (1983).
30. Royall, P. D., Delcourt, P. A. & Delcourt, H. R. Late quaternary paleoecology and paleoenvironments of the central Mississippi Alluvial Valley. *Geol. Soc. Am. Bull.* **103**, 157–170 (1991).
31. Hoadley, R. B. *Identifying Wood: Accurate Results With Simple Tools* (Taunton Press, 1990).
32. Fritts, H. *Tree Rings and Climate* (Elsevier, 1976).
33. Tucker, C. S. & Pearl, J. K. Coastal tree-ring records for paleoclimate and paleoenvironmental applications in North America. *Quat. Sci. Rev.* **265**, 107044 (2021).
34. Little, E. L. & Viereck, L. A. *Atlas of United States Trees* Vol. 5 (US Dept. of Agriculture, Forest Service, 1971).
35. Kennedy Jr, H. E. *Baldcypress: An American Wood (FS-218)* (US Dep. of Agriculture, Forest Service, 1972).
36. Conner, W. H. & Toliver, J. R. Long-term trends in the bald-cypress (*Taxodium distichum*) resource in Louisiana (USA). *For. Ecol. Manag.* **33**, 543–557 (1990).
37. Wilhite, L. & Toliver, J. *Taxodium distichum* (L.) rich. baldcypress. *Silv. N. Am.* **1**, 563–572 (1990).
38. Doyle, T. W., Chivoiu, B. & Enwright, N. M. *Sea-Level Rise Modeling Handbook: Resource Guide for Coastal Land Managers, Engineers, and Scientists* (US Department of the Interior, US Geological Survey, 2015).
39. Stahle, D. et al. Longevity, climate sensitivity, and conservation status of wetland trees at Black River, North Carolina. *Environ. Res. Commun.* **1**, 041002 (2019).
40. Keim, R. F. & Amos, J. B. Dendrochronological analysis of baldcypress (*Taxodium distichum*) responses to climate and contrasting flood regimes. *Can. J. For. Res.* **42**, 423–436 (2012).
41. Stahle, D. W. & Cleaveland, M. K. Reconstruction and analysis of spring rainfall over the southeastern US for the past 1000 years. *Bull. Am. Meteorol. Soc.* **73**, 1947–1961 (1992).
42. Stahle, D. W. et al. Tree-ring analysis of ancient baldcypress trees and subfossil wood. *Quat. Sci. Rev.* **34**, 1–15 (2012).
43. Hook, D. D. Waterlogging tolerance of lowland tree species of the south[1]. *South. J. Appl. For.* **8**, 136–149 (1984).
44. Middleton, B. A. & McKee, K. L. Use of a latitudinal gradient in bald cypress (*Taxodium distichum*) production to examine physiological controls of biotic boundaries and potential responses to environmental change. *Glob. Ecol. Biogeogr.* **13**, 247–258 (2004).
45. Shen, Z. et al. Rapid and widespread response of the Lower Mississippi River to eustatic forcing during the last glacial-interglacial cycle. *Bulletin* **124**, 690–704 (2012).
46. Gonzalez, S. et al. Facies reconstruction of a late Pleistocene cypress forest discovered on the northern Gulf of Mexico continental shelf. *Gulf Coast Assoc. Geol. Soc. Trans.* **67**, 133–146 (2017).
47. Rittenour, T. M. Luminescence dating of fluvial deposits: applications to geomorphic, palaeoseismic and archaeological research. *Boreas* **37**, 613–635 (2008).
48. Dalton, A. S., Stokes, C. R. & Batchelor, C. L. Evolution of the Laurentide and Innuitian ice sheets prior to the Last Glacial Maximum (115 ka to 25 ka). *Earth Sci. Rev.* **224**, 103875 (2022).
49. Delcourt, H. R. & Delcourt, P. A. Presettlement magnolia-beech climax of the Gulf Coastal Plain: quantitative evidence from the Apalachicola River Bluffs, north-central Florida. *Ecology* **58**, 1085–1093 (1977).
50. Wigley, T. M. L., Briffa, K. R. & Jones, P. D. On the average value of correlated time series, with applications in dendroclimatology and hydrometeorology. *J. Clim. Appl. Meteorol.* **23**, 201–213 (1984).
51. McVey, K. J. *Pleistocene and Early Holocene Aggradation of Mississippi River Tributaries Within Eastern and Western Lowlands of the Mississippi Alluvial Valley*. PhD thesis, University of Arkansas, Fayetteville (2005).
52. Rittenour, T. M. *Fluvial Evolution of the Lower Mississippi Valley Over the Last Glacial Cycle*. PhD thesis, The University of Nebraska-Lincoln (2004).
53. Rittenour, T. M., Goble, R. J. & Blum, M. D. Development of an OSL chronology for Late Pleistocene channel belts in the lower Mississippi Valley, USA. *Quat. Sci. Rev.* **24**, 2539–2554 (2005).
54. Rittenour, T. M., Blum, M. D. & Goble, R. J. Fluvial evolution of the lower Mississippi River Valley during the last 100 ky glacial cycle: response to glaciation and sea-level change. *Geol. Soc. Am. Bull.* **119**, 586–608 (2007).
55. Chabreck, R. H. *Vegetation, water and soil characteristics of the Louisiana coastal region (Bulletin No. 664)* (Louisiana State University and Agricultural and Mechanical College, Agricultural Experiment Station, 1972).
56. Pezeshki, S., DeLaune, R. & Patrick, W. Jr Flooding and saltwater intrusion: potential effects on survival and productivity of wetland forests along the US Gulf Coast. *For. Ecol. Manag.* **33**, 287–301 (1990).
57. Conner, W. H. The effect of salinity and waterlogging on growth and survival of baldcypress and Chinese tallow seedlings. *J. Coast. Res.* **10**, 1045–1049 (1994).
58. Javanshir, K. & Ewell, K. Salt resistance of bald cypress. in *Towards the Rational Use of High Salinity Tolerant Plants* 285–291 (Springer, 1993).
59. Krauss, K. W. et al. Site condition, structure, and growth of baldcypress along tidal/non-tidal salinity gradients. *Wetlands* **29**, 505–519 (2009).
60. Thomas, B. L., Doyle, T. & Krauss, K. Annual growth patterns of baldcypress (*Taxodium distichum*) along salinity gradients. *Wetlands* **35**, 831–839 (2015).
61. Harley, G. L., Maxwell, J. T. & Raber, G. T. Elevation promotes long-term survival of *Pinus elliottii* var. *densa*, a foundation species of the endangered pine rockland ecosystem in the Florida Keys. *Endang. Species Res.* **29**, 117–130 (2015).
62. Roche, D., Paillard, D. & Cortijo, E. Constraints on the duration and freshwater release of Heinrich event 4 through isotope modelling. *Nature* **432**, 379–382 (2004).

63. Denton, G. H. et al. The last glacial termination. *Science* **328**, 1652–1656 (2010).
64. Hemming, S. R. Heinrich events: Massive late Pleistocene detritus layers of the North Atlantic and their global climate imprint. *Rev. Geophys.* **42**, RG1005 (2004).
65. Conner, W. H, & Day, J. W. Jr. The effect of sea level rise on coastal wetland forests: the Mississippi Delta, USA, as a model. In *Coastally Restricted Forests* (ed. Laderman, A. D.) 278–292 (Oxford University Press, 1998).
66. Barrow, W. et al. Coastal forests of the Gulf of Mexico: a description and some thoughts on their conservation. in *Bird Conservation Implementation and Integration in the Americas: Proceedings of the Third International Partners in Flight Conference* (eds Ralph, C. J. & Rich, T. D.) 2002 March 20–24; Asilomar, CA, Vol. 1 Gen. Tech. Rep. PSW-GTR-191 (Albany, CA: US Dept. of Agriculture, Forest Service, Pacific Southwest Research Station: P., Vol. 191, 2005).
67. Heinrich, P. V. *Contrasting Pleistocene and Holocene Fluvial Systems of the Lower Pearl River* **37**, 41 (Louisiana and Mississippi, USA: Geological Society of America Abstracts with Programs, 2005).
68. Shen, H., Yu, L., Zhang, H., Zhao, M. & Lai, Z. OSL and radiocarbon dating of flood deposits and its paleoclimatic and archaeological implications in the Yihe River Basin, East China. *Quat. Geochronol.* **30**, 398–404 (2015).
69. Mobley, M. L., Richter, D. D. & Heine, P. R. Accumulation and decay of woody detritus in a humid subtropical secondary pine forest. *Can. J. For. Res.* **43**, 109–118 (2013).
70. Middleton, B. A. Differences in impacts of Hurricane Sandy on freshwater swamps on the Delmarva Peninsula, Mid-Atlantic Coast, USA. *Ecol. Eng.* **87**, 62–70 (2016).
71. Middleton, B. A. Effects of salinity and flooding on post-hurricane regeneration potential in coastal wetland vegetation. *Am. J. Bot.* **103**, 1420–1435 (2016).
72. Savard, M. M., B´egin, C., Marion, J., Arseneault, D. & B´egin, Y. Evaluating the integrity of C and O isotopes in sub-fossil wood from boreal lakes. *Palaeogeogr. Palaeoclimatol. Palaeoecol.* **348**, 21–31 (2012).
73. Esteban, L. G. et al. Softwood anatomy: a review. *Forests* **14**, 323 (2023).
74. Garretson, K. J. *Analysis of Fossil Pollen From a Pleistocene Cypress Forest Preserved on the Northern Gulf of Mexico Continental Shelf*. University of Southern Mississippi (2022).
75. G¨artner, H. & Nievergelt, D. The core-microtome: a new tool for surface preparation on cores and time series analysis of varying cell parameters. *Dendrochronologia* **28**, 85–92 (2010).
76. Von Arx, G., Crivellaro, A., Prendin, A. L., C˘ufar, K. & Carrer, M. Quantitative wood anatomy—practical guidelines. *Front. Plant Sci.* **7**, 781 (2016).
77. Stokes, M. A. & Smiley, T. L. *An Introduction to Tree-Ring Dating* (University of Chicago Press, Chicago, IL, 1968).
78. Larsson, L. CooRecorder and Cdendro programs of the CooRecorder/Cdendro package version 7.7 (2014).
79. Holmes, R. L. Computer-assisted quality control in tree-ring dating and measurement. Tree-Ring Bull. **43**, 69–78(1983).
80. Cook, E. & Kairiukstis, L. (eds) *Methods of Dendrochronology: Applications in the Environmental Sciences* (Kluwer Academic, Doredrecht, 1990).
81. Stahle, D. W., Therrell, M. D. & Cleaveland, M. K. NOAA/WDS Paleoclimatology - Stahle - Pascagoula River - TADI - ITRDB MS002. NOAA National Centers for Environmental Information. https://doi.org/10.25921/8m97-kz34 (2002).
82. Biondi, F., Qeadan, F. & Theory-Driven, A. Approach to tree-ring standardization: defining the biological trend from expected basal area increment. *Tree Ring Res.* **64**, 81–96 (2008).
83. Bunn, A. G. A dendrochronology program library in r (dplR). *Dendrochronologia* **26**, 115–124 (2008).
84. Torrence, C. & Compo, G. A practical guide to wavelet analysis. *Bull. Am. Meteorol. Soc.* **79**, 61–78 (1998).
85. Grinsted, A., Moore, J. C. & Jevrejeva, S. Application of the cross wavelet transform and wavelet coherence to geophysical time series. *Nonlinear Process. Geophys.* **11**, 561–566 (2004).
86. Gu, S. et al. Assessing the ability of zonal δ18o contrast in benthic foraminifera to reconstruct deglacial evolution of Atlantic Meridional Overturning Circulation. *Paleoceanogr. Paleoclimatol.* **34**, 800–812 (2019).
87. Railsback, L. B., Gibbard, P. L., Head, M. J., Voarintsoa, N. R. G. & Toucanne, S. An optimized scheme of lettered marine isotope substages for the last 1.0 million years, and the climatostratigraphic nature of isotope stages and substages. *Quat. Sci. Rev.* **111**, 94–106 (2015).
88. Heinrich, H. Origin and consequences of cyclic ice rafting in the northeast Atlantic ocean during the past 130,000 years. *Quat. Res.* **29**, 142–152 (1988).

Acknowledgements

Funding for this study was provided by the US Department of the Interior, Bureau of Ocean Energy Management (BOEM), Environmental Studies Program, Washington, DC, under Agreement Numbers M20AC10002 and M15AC00016. We also would like to thank the Wallace Research Foundation for providing initial funding. We thank the Field Support Group of the Coastal Studies Institute at LSU for their assistance in field operations. A special thank to Tom Guilderson of the Center for Accelerator Mass Spectrometry, Lawrence Livermore National Laboratory for his help with radiocarbon dating analysis and interpretations, as well as Zhixiong Shen for facilitating OSL dating. We deeply thank Ben Raines for his local knowledge of the site and support of our investigation of the Underwater Forest. We thank the anonymous reviewers for taking the time to offer suggestions that improved earlier drafts of this manuscript. This report has been technically reviewed by BOEM, and it has been approved for publication. The views and conclusions contained in this document are those of the authors and should not be interpreted as representing the opinions or policies of the Bureau of Ocean Energy Management. Mention of trade, firm, or product names does not constitute their endorsement or recommendation for use by the US government.

Author contributions

G.H. and K.D. conceptualized the research and designed the study methodology. Data collection and fieldwork were conducted by G.H., K.D., C.R., S.B., K.X., K.M., and A.C., with assistance from M.L., E.B., and K.K., who helped process and analyze the data. The initial manuscript draft was prepared by G.H. and K.D., with revisions and critical feedback provided by all other authors. All authors reviewed, edited, and approved the final manuscript.

Competing interests

The authors declare no competing interests.

Additional information

Supplementary information The online version contains supplementary material available at https://doi.org/10.1038/s41612-025-00951-y.

Correspondence and requests for materials should be addressed to Grant L. Harley.